JI, F.-Z., BARATI, M., COLY, K., and IRONS, A.G. A kinetic study of carbon injection into electric arc furnace slags. *VII International Conference on Molten Slags Fluxes and Salts,* The South African Institute of Mining and Metallurgy, 2004.

# A kinetic study of carbon injection into electric arc furnace slags

F.-Z. JI, M. BARATI, K. COLEY, and A.G. IRONS
*Department of Materials Science and Engineering, McMaster University, Hamilton, Ontario, Canada*

In order to optimize carbon injection into oxidizing slags, in terms of carbon and iron yield, we must have a detailed understanding of the kinetics of the reactions involved. The current study measures the rate of carbon oxidation during injection at steelmaking temperature by means of injections of coal into EAF slags. The compositions of analysed outgoing gas were used to calculate gas flow rate and hence the gasification rate of carbon. A fundamental equation to predict residual carbon in slags was developed. The predictions using this model at moderate injection rates are in good agreement with experimental data. The reaction rate of EAF slag with carbon is under mixed control by the slag gas and the gas carbon reactions. The relative importance of each step depends mainly on the v-ratio of slags. A relative reactivity parameter $\chi$ has been defined and it is found to be important to carbon-slag reaction kinetics and slag foaming.

Key words: carbon-slag reaction, kinetics, slag foaming.

## Introduction

Slag foaming has been extensively studied because of its importance in many pyrometallurgical processes[1–2]. In the case of coal injection into slags, the reduction of iron oxides will generate a large number of bubbles. This will result in slag foaming and, at the same time, some iron in the slag will be recovered. For the EAF process, a stable foamy slag is essential to save electrical energy, protect the furnace lining, decrease noise and electrode consumption. To control the slag foaming and reduction of slag by carbon injection, one has to understand the kinetics of the slag-carbon reaction. The reaction between carbon and slag as show in Figure 1 includes four separate steps: iron cations transfer from the bulk slag phase to the slag-gas interface, CO reacts with oxygen in the slag, $CO+O^{2-}= CO_2+2e$, $CO_2$ transfer through the gas phase to the surface of carbon and $CO_2$ reaction with carbon to form CO. These processes involve gas-liquid, gas-solid and even solid-liquid reactions, as well as mass transfer in the gas and slag phases. To understand those phenomena, a number of authors have studied reduction behaviour of iron oxides thermodynamically and kinetically[3–7]. For the reaction between carbon and CO+ $CO_2$ gas, Turkdogan gave a detailed description of the reaction rate for different carbonaceous materials. Fruehan *et al.*[9] reported the kinetics of oxidation of carbonaceous materials by $CO_2$ and $H_2O$. To clarify the reaction kinetics and find the optimum conditions of coal injection into slags, experiments of coal injection directly into slags were carried out in the present study. On the basis of kinetic analysis, slag foaming is discussed as well.

## Experimental

Experiments were carried out in a 75 kW induction furnace. High-MgO crucible with interior diameter of 191 mm and height of 295 mm about 65 kg liquid steel capacity was used for the experiments. Figure 2 shows the experimental set up. Nitrogen was passed through a digital flow meter then introduced into the feeder for coal injection. The feeder was suspended from a load cell to monitor the injection quantity of coal. The pressure in the feeder was measured using a pressure transducer installed on the cover of the feeder. Before coal injection started, the crucible was covered with a ceramic fibreboard and a stainless steel lid. The injection lance was introduced into the crucible through holes in the centre of the lid and the ceramic fibreboard.

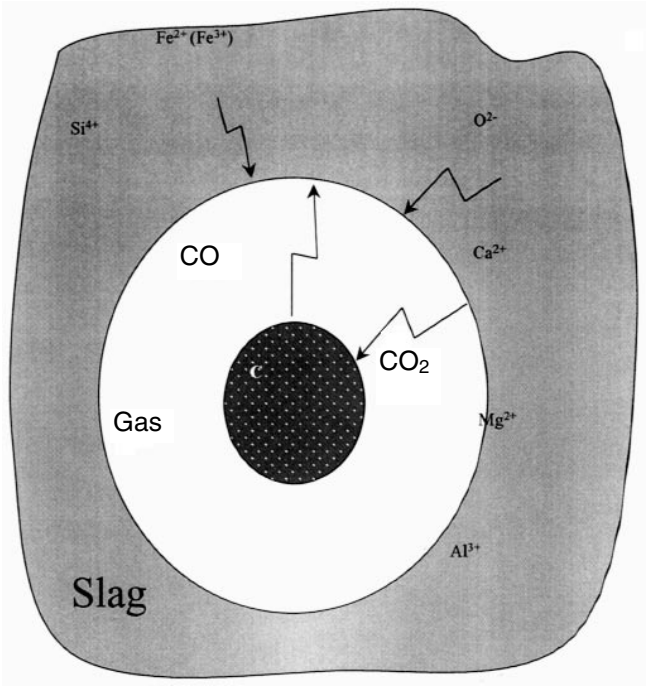


**Figure 1. Schematic of carbon-slag reaction**

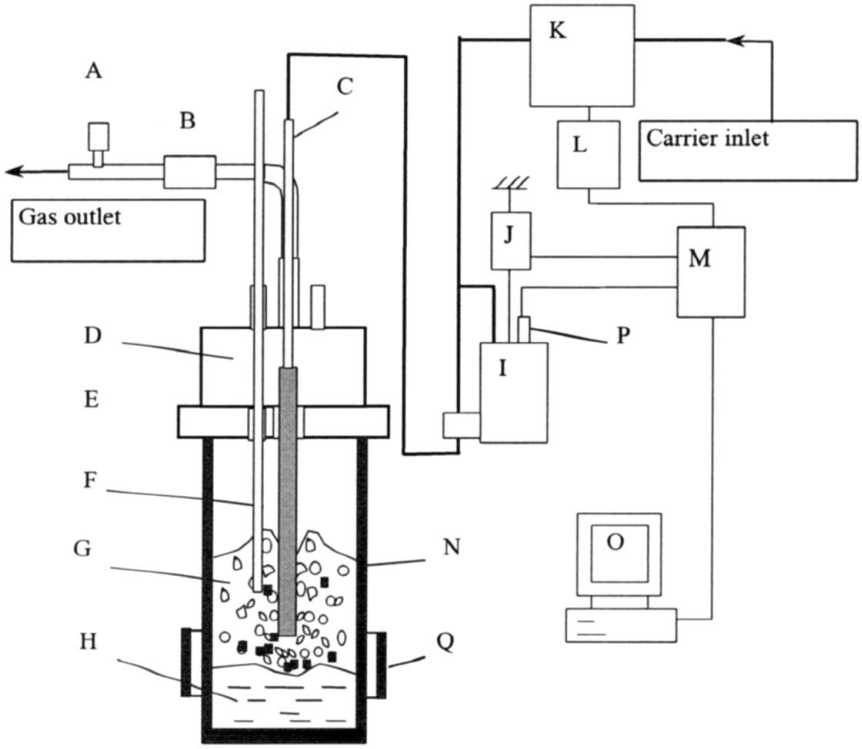


A-Gas sample port; B-filter; C-Lance; D-lid; E-Ceramic fibreboard; F-Steel rod; G-Slag: H-Steel; I-Feeder; J-Load cell; K-Flow rate transducer; L-Flow meter; M-A/D card terminal; N-High-MgO crucible; O-Computer; P-Pressure transducer; Q-Graphite ring

**Figure 2. the experimental setup**

During experiments, the gas was exhausted through a single outlet. To take gas samples, a special port was mounted on the outgoing gas line and the gas samples were withdrawn using gas tight syringes. A filter fitted with a fine screen and glass wool was used for collecting the dust. The signals of carrier gas flow rate, internal pressure of the feeder and weight of coal were collected by a computer at 0.5 second intervals. Detailed experimental materials and procedures please refer to the previous publication[10].

## Description of kinetics

### Flow rate of gas

In the present study, gas flow rate is a key factor to determine gasification rate of carbon in slag and foaming height. The gas flow rates were calculated based on gas compositions and the flow rate of carrier gas (nitrogen). To calculate the flow rate of gas generated initially in the slag by carbon slag reaction, one has to convert the analysed gas composition to that before post combustion. To do so, the variation of carbon dioxide after post combustion has to be know, i.e.

$$\Delta\%CO_2 = \%CO_2 - \%CO_{2\chi} \quad [1]$$

Where, $\Delta\%CO_2$ is the additional $CO_2$ arising from post combustion. The $\%CO_{2\chi}$ depends on reaction rates of the slag-gas and gas-carbon. In the present study where the reaction time is relatively short, equilibrium can not be reached at both interfaces. Hence the partial pressure of carbon dioxide in the gas halo should be somewhere between the two equilibrium partial pressures of the reactions gas-slag ($CO+FeO=CO_2+Fe$, $P_{CO2a}$) and gas-carbon ($CO_2+C=2CO$, $P_{CO2b}$) and close to the faster. Assuming the gas is ideal and uniform, the following equation can be used to determine $\%CO_{2\chi}$,

$$\%CO_{2\chi} = P_{CO_2\chi} = \chi P_{CO_2 a} + (1-\chi) P_{CO_2 b} \quad [2]$$

Where, obviously, the value of $\chi$ should be between 0 for slow slag reduction and 1 for slow carbon gasification and it should be greater than 1 if $Fe_2O_3$ is present in the slag. The equilibrium partial pressure of $CO_2$ for gas-slag reaction is a function of temperature and activity of iron oxide in the slag. On the gas-carbon interface, the equilibrium partial pressure of $CO_2$ is a constant at given temperature and carbonaceous material.

To determine the value of $\chi$, one has to find the reaction rates of these two reactions experimentally. However, prior to determining the rate controlling steps, $P_{CO2\chi}$ can be approximated by properly choosing $\chi$ values to close the carbon balance. In this way, one can also evaluate the rate limiting step.

Based on the gas composition, using nitrogen and oxygen balances, the initial flow rate of CO and $CO_2$ and air entrained can be calculated. Detailed calculations have been described in the earlier publication[10]

### Carbon gasification and balance

The gasification rate of carbon in slags in g/s can be estimated using flow rate of CO and $CO_2$ mentioned earlier. It should be noted that this gasified carbon includes carbon gasification in slags and that of carbon floating on the slag surface. At any instant, residual carbon in the slag should

be equal to carbon injected minus carbon gasified and escaped to outgoing gas as dust as well as dissolved in the steel. Figure 3 shows an example of the carbon balances and residual carbon. It can be seen that 2 minutes after the injection stopped, carbon gasification is essentially completed. This is determined from the gas analysis so must be consistent. The value of $\chi$ in Figure 3[10] was determined as follows.

To find the best fitting value of $\chi$, several $P_{CO2\chi}$ were calculated by inserting different values of $\chi$ in Equation [2]. With the different $P_{CO2\chi}$, the difference in weight between carbon injected and consumed was found. When one of the $\chi$ values makes a difference of less than ±0.3 grams, the balance of carbon is considered to be achieved. In this way, the value of $\chi$ was found to be 0.91 for injection[9]. For other experiments, $\chi$ were determined by the same method.

**Kinetic model and discussion**

According to carbon balance, the accumulation rate of carbon in slag is expressed as follows,

$$\frac{dw}{dt} = R_i - \left(k + k_f + k_s + k_e\right) \cdot w \qquad [3]$$

During coal injection $0 \le t \le t_i$ and $R_i > 0$, where, w is the quantity of coal in slag in gram, t the time in second, $t_i$ the coal injection termination time, $R_i$ the injection rate of coal in g/s, k the apparent first order rate constant of carbon reacted with CO-$CO_2$ gas, $k_f$ the rate constant for flotation of coal, $k_s$ the rate constant for dissolution in steel and $k_e$ the rate constant for escape of carbon in the outgoing gas. As noted earlier, the maximum value of carbon dissolved in steel and dust collected from the outgoing gas was about 0.97% of the total carbon injected and we can also suppose the carbon settled in the lid and conveying line is very small, thus the $k_s$ and $k_e$ are considered negligible.

After coal injection stops, i.e. $t_i \le t \le t°$ and $R_i = 0$, the accumulation rate of carbon in slag is:

$$\frac{dw}{dt} = -\left(k + k_f\right)w \qquad [4]$$

It should be noted that this represents a negative accumulation. Because the coal particles are small in the present experiments, complete pore diffusion can be assumed. Supposing the rate constant for metallurgical coke is reasonable for the low volatile coal used in the present experiments, the reaction rate constant k reported by Turkdogan can be used[8]. Figure 4[10] shows good agreement between predicted and measured residual carbon for injections with very different values of $\chi$. In general, the predicted maximum in residual carbon is slightly higher than experimental. On the other hand, a strong positive relation between coal injection rate and gasification rates can be found as shown in Figure 5. Accordingly, these suggest that there should be an injection saturation point when:

$$k_c A_c \left(\Delta CO_2\right)_{carbon} > k_s A_s \left(\Delta CO\right)_{slag} \qquad [5]$$

Where, $k_G$, $A_G$ are rate constant and surface area at carbon-gas interface respectively, and $k_s$ and $A_s$ are the same at

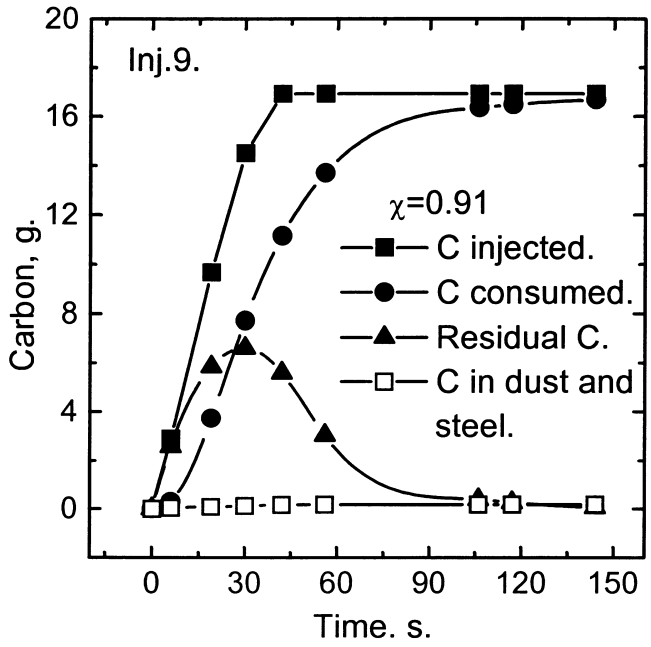


**Figure 3. Carbon balances for the injection 9[10]**

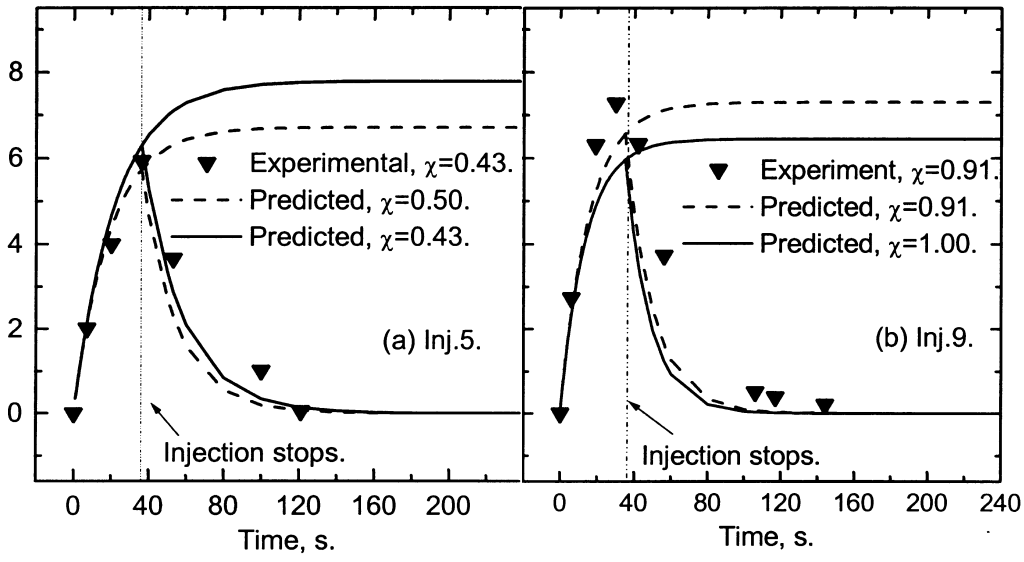


**Figure 4. Comparison between predicted and experimental residual carbon for (a) Injection No. 5 and (b) Injection No. 9[11]**

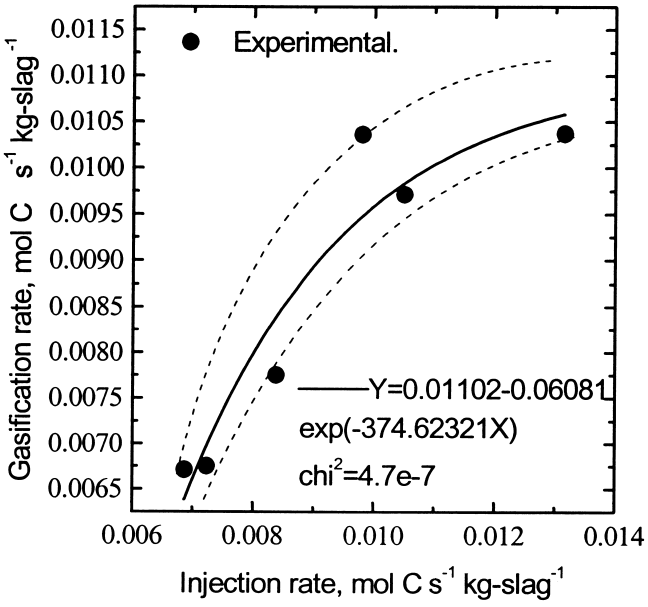


**Figure 5. Relationship between gasification rates and injection rates of carbon**

slag-gas interface. The $(\Delta CO_2)_{carbon}$ and $(\Delta CO)_{slag}$ are the differences of $CO_2$ and CO in the bubbles and equilibrium with the carbon and slag interface respectively. This saturation point depends on the number of particles per bubble or combination of injection rate and slag and carbon reactivity. Before this point, the gasification rate of carbon mainly depends on injection rate and after this point the rate will be decided by either reaction ability of slag or carbon reaction rate.

To be able to predict the reaction rates between carbon and slag using only outgoing gas information, one has to know the values of $\chi$ for estimating initial carbon dioxide in the gas halo. Application of multi regression method to the experimental data from the six injections, an empirical equation of $\chi$ as a function of both FeO′ and B1 is obtained[11].

$$\chi = 1.296 - 3.153 \cdot \exp(-0.701 \cdot B1) + 86.12 \cdot \exp(-0.216 \cdot \%FeO') \quad R^2 = 0.97 \qquad [6]$$

Figure 6 shows a comparison between calculated curves using Equation [6] and experimental values. It is found that the effect of FeO′ on $\chi$ is small relative to basicity. At higher basicity the reactivity of the slag increases. Similarly, increasing FeO in the slag also increases basicity but lesser extent than CaO and MgO. On the other hand, under higher basicity, the effect of FeO on $\chi$ is slightly greater than lower basicity. In our calculations only the oxidizing effect of FeO is considered. Therefore, increasing $Fe^{3+}$ will provide unaccounted for oxidizing power, thereby increasing the apparent value of $\chi$. If the $Fe^{3+}$ content had been considered in calculating $P_{CO2a}$, the variation in $\chi$ would only be due to kinetic effects and would be expected to be higher at lower $Fe^{3+}$. Yang and Belton[12] propose the relationship between the ratio of ferric to ferrous ions with $(CaO+MgO)/SiO_2$ and $P_{CO2}/P_{CO}$ as follows,

$$\log\left(\frac{Fe^{3+}}{Fe^{2+}}\right) = 0.3(\pm 0.02)\frac{CaO+MgO}{SiO_2} + 0.45(\pm 0.01)\log\left(\frac{P_{CO2}}{P_{CO}}\right) - 1.24(\pm 0.01) \qquad [7]$$

This equation indicates that at constant $P_{CO2}/P_{CO}$, logarithm of the ratio of ferric to ferrous ions is proportional to $(CaO+MgO)/SiO_2$.

The results of this study are consistent with Equation [7][12] and Turkdogan's studies[8a], in these publications they found that when slag basicity rises, the ionic ratio of ferric to ferrous increases. Obviously, the reaction limiting step is carbon gas reaction for this case. When B1 lies between 1.8 and 3.1, $0.5<\chi<1$, reactions at the slag-gas and gas-carbon interface both play a role in controlling the rate with the slag gas reaction being faster. While B1<1.8, $\chi<0.5$, the rate of carbon gas reaction will be faster.

## Slag foaming

A number of researchers have studied foaming behaviour of various slags. Void fraction (gas hold-up) according to Guo *et al.*[13] is,

$$\frac{\alpha^2}{(1-\alpha)} = 0.91 u_s^{0.57} \qquad [8]$$

The foaming height can be obtained using the equation suggested in reference [13]:

$$h_f = \frac{h_s}{(1-\alpha)} \qquad [9]$$

where $h_s$ is static depth of slag. Following expressions (8) and (9), the void fractions and foaming heights of slags can be calculated. The foaming Index reported by Jiang and Fruehan[14] is:

$$\sum = \frac{115\mu}{(\rho\sigma)^{0.5}} = \frac{h_f}{u_2} \qquad [10]$$

where $\mu$ is viscosity, $\rho$ the density and $\sigma$ the surface tension of slag, the $h_f$ and $u_s$ are slag foaming height and superficial gas velocity respectively. For the present studies, the superficial gas flow rate can be obtained by the flow rate of $CO+CO_2$ and carrier gas divided by crucible section area. Table I lists the main experimental results and superficial gas velocity calculated using gas flow rate and section area of the crucible.

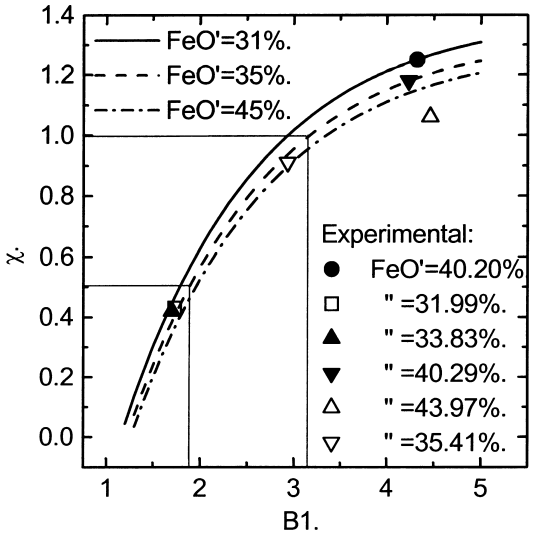


**Figure 6. $\chi$ as a function of basicity [B1=(%CaO+%MgO)/(%$Al_2O_3$+%$SiO_2$)] with different FeO′ content**

**Table I**
**Main experimental results and superficial gas velocity**

| | Steel | | Slag | | Coal injection | | t, (°C) | Us (ms$^{-1}$) | FeO' (mass%) | B1 |
|---|---|---|---|---|---|---|---|---|---|---|
| | W (kg) | Dep. (mm) | W (kg) | Deep (mm) | $W_{coal}$ (g) | Rate (mol C s$^{-1}$ kg-slag$^{-1}$) | | | | |
| Inj 4 | 17.05 | 98.4 | 5.49 | 44.5 | 37.71 | 0.01315 | 1667 | 0.287 | 40.20 | 4.32 |
| Inj 5 | 16.94 | 92.1 | 4.42 | 57.2 | 13.84 | 0.00724 | 1673 | 0.167 | 31.99 | 1.73 |
| Inj 6 | 17.54 | 104.8 | 5.09 | 54.0 | 18.04 | 0.00687 | 1687 | 0.181 | 33.83 | 1.70 |
| Inj 7 | 17.28 | 98.4 | 4.86 | 41.3 | 19.31 | 0.00838 | 1593 | 0.198 | 40.29 | 4.23 |
| Inj 8 | 16.54 | 101.6 | 4.49 | 41.3 | 16.95 | 0.0105 | 1702 | 0.226 | 43.97 | 4.46 |
| Inj 9 | 16.90 | 111.1 | 4.62 | 41.3 | 19.00 | 0.0098 | 1691 | 0.241 | 35.41 | 2.93 |

Figure 7 shows the comparison of predicted void fractions by different authors[13,15,16] and the present experimental data. The experimental data from the present work are located in the left top corner, which means the slag foaming is still in the low superficial gas velocity region or conventional regime[13].

Figure 8 gives the relationship of slag foaming heights and superficial gas velocities calculated by foaming index reported by Fruehan *et al.*[14]. The viscosities of slags in the present experiments are between 0.04–0.12 Pa·s. According to Birkman[17]

$$\mu = \mu_f(1+5.5\varepsilon) \qquad [11]$$

The percentage of solid particles ε causes increased effective viscosities. If we assume ε to be 0.2 and the viscosities of slags and foaming indexes can be recalculated shown in Figure 8. These current experimental points are placed in the Figure for comparison. It can be found that the deviations between experimental and predicted values seem to be acceptable. Detailed analyses are ongoing. It should be mentioned that the results reported by Fruehan were for lower superficial gas velocities (less than 0.05m/s, dash dot line box in Figure (4)[14]. Guo *et al.* hold fits better for high superficial gas velocities and theory of Fruehan *et al.* is better at low. However, the present conditions appear to be in an intermediate regime, where neither model fits perfectly.

In the analysis of the present experimental data, no simple relation was found between void fraction and superficial gas velocity that is shown in Figure 9. However, a smooth relation was found between void fraction and χ which is shown in Figure 10. According to Figure 10, an empirical equation between void fraction and χ was found as follows:

$$\alpha = 1.06855 - 1.29785_{\chi} + 0.87053_{\chi}^{2} \qquad [12]$$

χ can be expressed as a function of basicity and FeO' using Equation [6]. Combination of Equations [12] and [6] yields void fraction as a function of B1 and FeO' shown in Figure (11). Figure 11 demonstrates that the v-ratio plays an important role in slag foaming. It is reasonable to expect foaming to follow the trend shown in Figure 11. When basicity increases, the viscosity of slag decreases dramatically. Therefore the foaming ability of slag decreases significantly as shown in Figure 11. When v-ratio is over 2.5 to 3.0, the increase of viscosity of slag is mainly due to melting point rising and some solid particles forming. However, the remarkable correlation shown in Figure 10 between void fraction and χ is not so readily explained. χ is a relative reactivity parameter that reflects the relative rates of reaction at the carbon gas and slag gas interfaces. Perhaps the strong correlation is obtained

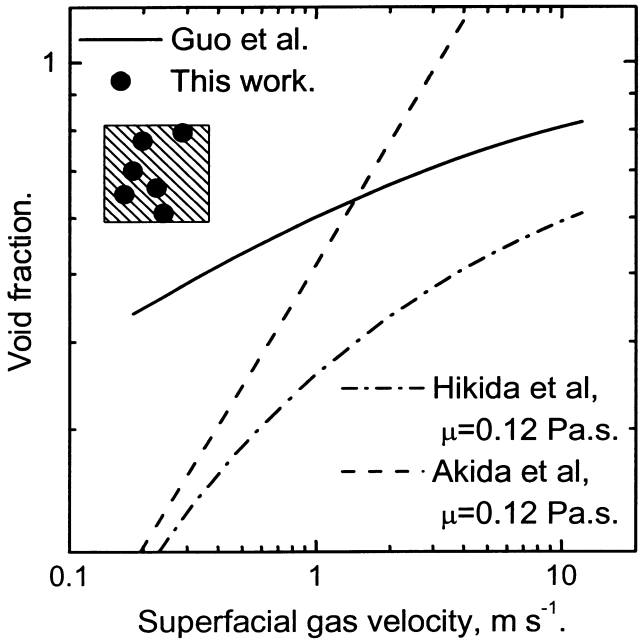


**Figure 7. Slag void fractions as a function of superficial gas velocity[13,15–16]**

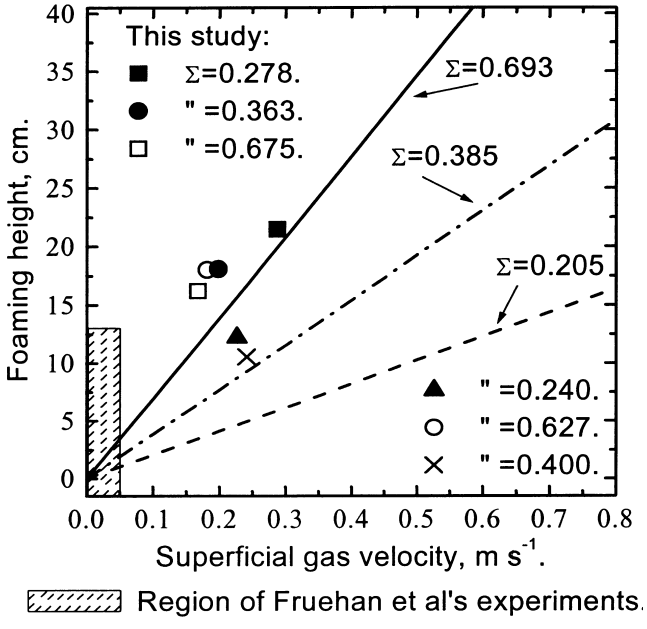


**Figure 8. Foaming height as a fraction of superficial gas velocity**

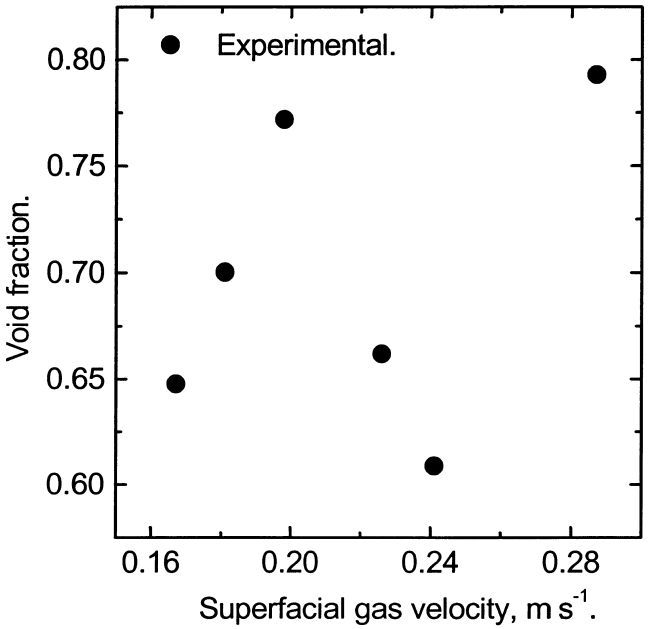


**Figure 9. Void fraction as a function of superficial gas velocity**

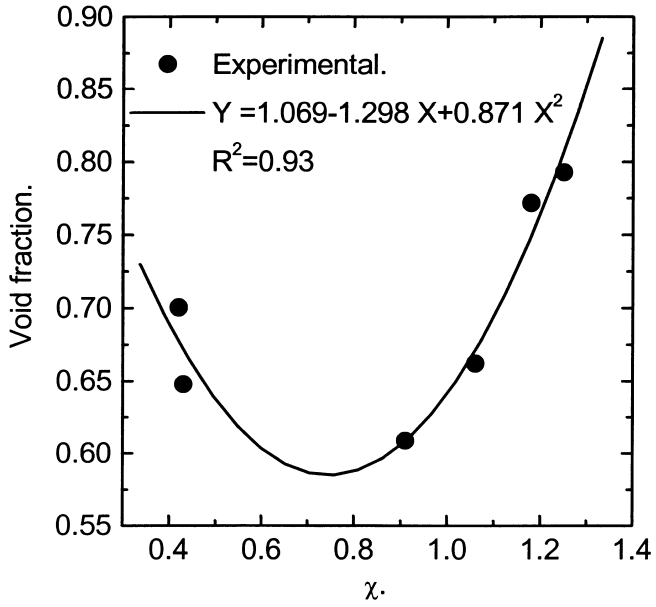


**Figure 10. Void fraction as a function of χ**

because χ embodies a number of parameters that affect foaming; it reflects bubbles size and is a measure of slag reactivity and, therefore, superficial gas flow rate. Work is ongoing to establish a formal relationship between χ and void fraction of foaming slag.

Here a primary analysis is as follows. As well known, slag void fraction can also expressed as,

$$\alpha = \frac{Qg}{u_b A} \quad i.e., \quad u_b = \frac{Qg}{\alpha A} \qquad [13]$$

Hence, we can estimate the bubble diameter using following relationship,

$$u_b = \frac{g d_b^2 \Delta\rho}{18\mu} \qquad [14]$$

Where α is void fraction, $Q_g$ the gas flow rate, $u_b$ the bubble rising terminal velocity, A the crucible section area, g the acceleration due to gravity, $d_b$ the bubble diameter and Δρ the difference of density between slag and gas. Equation [14] is valid when $d_b \leq 0.2$ cm and $Re_b \leq 1$. The bubble Reynolds number[18] is.

$$Re_b = \frac{d_b u_b \rho 1}{\mu_1} \qquad [15]$$

The rise velocity and diameters of the bubbles for the present work were calculated using Equations [13] and [14] and found to be 0.028 to 0.046 m/s and 1.0 to 1.4 mm respectively. Then, according to Equation [15], the $Re_b$ =0.96–2.99, hence the bubble motion should essentially obey Stokes' law[18]. This confirmed the availability of Equation [14] in this study.

Figure 12 shows a relationship between bubble size and χ. A regression equation between $d_b$ and χ is also shown in this Figure. When χ is less than 0.8, it does not affect bubble size significantly but when χ is greater than 0.8, it makes bubbles smaller. This is helpful to keep slag foam stable, in general.

## Conclusions

- Reaction rate of low volatile coal with EAF slag at moderate injection rate of coal can be approximated using a published rate constant for metallurgical coke and an appropriately chosen value for the relative reactivity parameter. The maximum gasification rate of carbon in slags was found to be in the range 0.006–0.011 mole C $s^{-1}$ kg-$slag^{-1}$ and the gasification rate strongly depends on the injection rate of coal for lower injection rates
- The effect of basicity on the slag-gas reaction rate constant dominates relative to iron oxide content. For basicity of slags greater 3.2, the rate-limiting step is the carbon-gas reaction. When the v-ratios between 1.8 and 3.2, reactions at the slag-gas and gas-carbon interface both play a role in controlling the rate with the slag gas reaction being faster. When the basicity is lower than 1.8, the carbon-gas reaction is faster

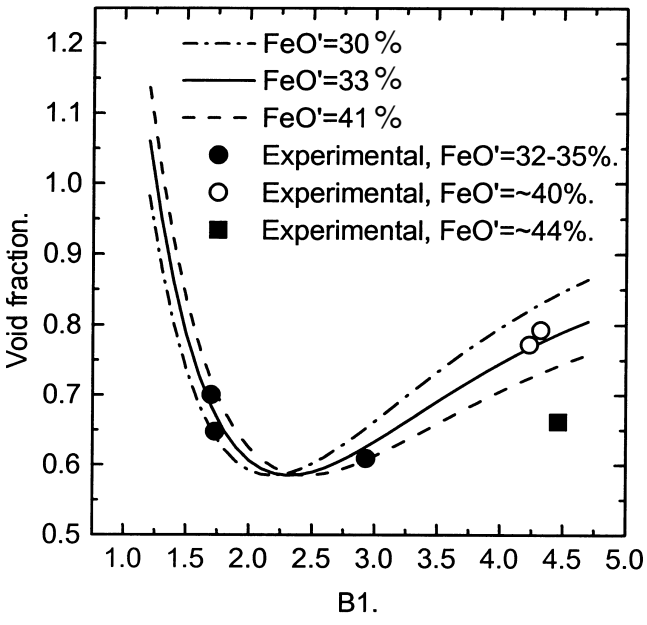


**Figure 11. Void fraction as a function of basicity [B1 = (%CaO+MgO)/(%$Al_2O_3$+%$SiO_2$)] and FeO′%**

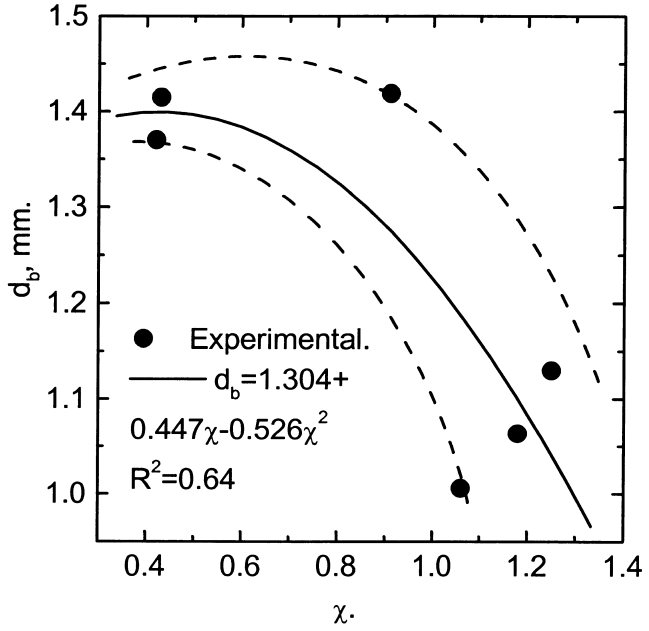


**Figure 12. Bubble size as a function of χ**

- The value of χ is an important parameter for carbon slag reaction and slag foaming because it reflects a number of parameters important in slag foaming.

## Acknowledgements

The authors are deeply grateful to McMaster Steel Research Centre and its Industrial Members for funding this work, to Dofasco for the kind help with experimental materials and chemical analysis, and also to O. Kelly, G. Bishop, D. Angelina and Subagyo for great cooperation during the experiments. Assistance with gas chromatograph operation from E. Worral is gratefully acknowledged.

## References

**1.** JUNG, S. and FRUEHAN, R.J. Foaming Characteristics of BOF Slags, *59th Ironmaking Conference Proceedings*, Pittsburgh, Pennsylvania, March 26–29, ISS, USA, 2000. pp. 517–527.

**2.** HARA, S. AND OGINO, K. Slag Foaming Phenomenon in Pyrometallurgical Processes, *ISIJ Int.*, vol. 32, 1992, pp. 81–86.

**3.** DARKEN, L.S. and GURRY, R.W. The system Iron-Oxygen II. Equilibrium and Thermodynamics of Liquid Oxides and Other Phases, *J. Am. Chem. Soc.*, vol. 68, 1946, pp. 798–816.

**4.** KIM, S.-Y. and SONG, B. Thermodynamic Aspects of Steel Reoxidation Behaviour by the Ladle Slag system of CaO-MgO-$Al_2O3$-$Fe_tO$-MnO-$P_2O_5$, Metall. *Mater. Trans. B*, vol. 30B, 1999, pp. 435–442.

**5.** BYGDEN, J., SICHEN, D., and SEETHARAMAN, S. Thermodynamic Description of 'FeO'-MgO-$SiO_2$ and 'FeO'-MnO-$SiO_2$ *Melts- a Model Approach, Steel Research*, vol. 65, 1994, pp. 421–428.

**6.** SEO, J. and KIM, S. Reaction Mechanism of FeO Reduction by Solid and Dissolved Carbon, *Steel Research*, vol. 69, 1998, pp. 306–310.

**7.** SAIN, D.R. and BELTON, G.R. Interfacial Reaction Kinetics on the Decarburization of liquid Iron by Carbon Dioxide, *Metall. Trans. B,* vol. 7B, 1976, pp. 235–244.

**8.** TURKDOGAN, E.T. *Fundamental of Steelmaking*, The University Press, Cambridge, UK, 1996, pp. 51–57; a: p. 165.

**9.** STORY, S.R. and FRUEHAN, R.J. Kinetics of Oxidation of Carbonaceous Materials by $CO_2$ and $H_2O$ between 1300°C and 1500°C, *Met. Mat. Trans. B*, vol. 31B, 2000, pp. 43–54.

**10.** JI, F.-Z., BARATI , M., COLEY, K., and IRONS, G. A. *Proceedings of ISS TECH 2003 Conference*, *Indianapolis*, IN, USA, Apr. 27–30, 2003, pp. 703–711.

**11.** JI, F.-Z., BARATI , M., COLEY, K., and IRONS, G. A. Kinetics of Coal Injection into Iron Oxides Containing Slags, submitted to *ISIJ International* For publication.

**12.** YANG, L. and BELTON, G.R. Iron redox equilibria in CaO-$Al_2O_3$-$SiO_2$ and MgO-CaO-$Al_2O_3$-$SiO_2$ slags, *Met. Mat. Trans. B*, vol. 29B, 1998, pp. 837–845.

**13.** GUO, H., IRONS, G.A., and LU, W.-K. A Multiphase Fluid Mechanics Approach to Gas Holdup in Bath Smelting Processes, *Met. Mat. Trans*. vol. 27B, 1996, pp. 195–201.

**14.** JIANG, R. and FRUEHAN, R.J. Slag Foaming in Bath Smelting, *Metall. Trans. B*, vol. 22B, 1991, pp. 481–489.

**15.** AKITA, K. and YOSHIDA, F. Gas Holdup and Volumetric Mass Transfer Coefficient in Bubble Columns, *Ind. Eng. Chem. Process. Des. Dev*. vol. 33, 1973, pp. 76–80.

**16.** HIKITA, H., ASAI, S., TANIGAWA, K., SEGAWA, K., and KITAO, M. Gas Hold-up in Bubble Columns, *Chem. Eng. J*., 1980, vol. 20, pp. 59–67.

**17.** BIRKMAN, H.C. The viscosity of concentrated solutions and suspensions, *J. Chem. Phys*., vol. 20, 1952, p. 571.

**18.** DEO, B. and BOOM, R. Fundamentals of Steelmaking Metallurgy, *Prentice Hall International, Hertfordshire*, UK, 1993, p. 5.